MASTER

LBL-9992

CONF-791057--

Lawrence Berkeley Laboratory
UNIVERSITY OF CALIFORNIA

Accelerator & Fusion Research Division

To be published in the Proceedings of the Workshop on
Hydrogen Recycling, Dublin, CA, October 17-18, 1979

NEGATIVE-HYDROGEN-ION PRODUCTION BY BACKSCATTERING FROM ALKALI-METAL TARGETS

P. J. Schneider, K. H. Berkner, W. G. Graham,
R. V. Pyle, and J. W. Stearns

November 1979

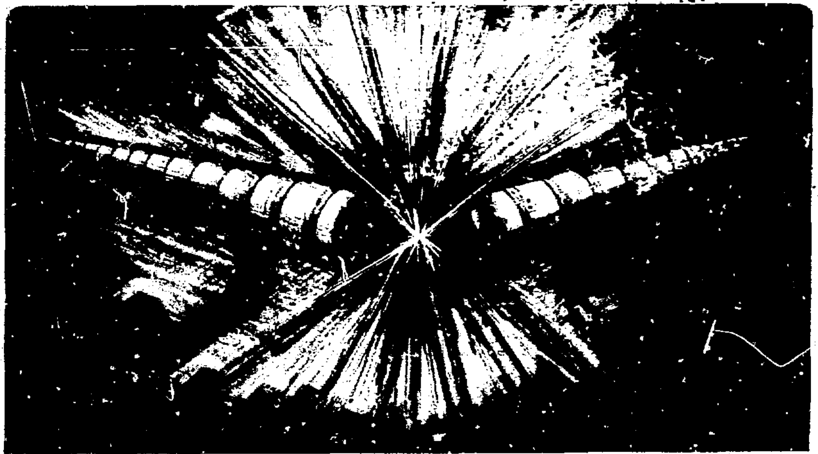

Prepared for the U.S. Department of Energy under Contract W-7405-ENG-48

LBL-9992

Negative-Hydrogen-Ion Production by Backscattering from Alkali-Metal Targets*

P. J. Schneider, K. H. Berkner, W. G. Graham, R. V. Pyle, and J. W. Stearns

Lawrence Berkeley Laboratory, University of California
Berkeley, California 94720

Measurements have been made of the total backscattered D^- and H^- yields from Cs, Rb, K, Na and Li surfaces bombarded with D_2^+, D_3^+, H_2^+ and H_3^+ in the energy range 0.15 to 4 keV/nucleus. All measurements were made at a background pressure less than 10^{-9} Torr and the alkali-metal surfaces were evaporated onto a substrate in situ to minimize contamination of surfaces. For each target, the D^- and H^- yields exhibited maxima (as high as 8% per incident deuteron or proton for Cs); the maxima occurred at incident energies between 300 and 1000 eV/nucleus and always occurred at a lower incident energy for H than for D for a given target. Both the H^- and D^- yields decreased, at any measured energy, in going from Cs to Li in the order given above.

Measurements of the H^- yield were also made for H_3^+ bombarding a W substrate, as a function of the work function of the target, as Li was deposited on the W. The work function of the target showed a minimum as the Li coverage was increased and the H^- yield showed a corresponding maximum which was almost two orders of magnitude higher than the H^- yield for a thick Li target.

Apparatus and Procedure

A beam of H_2^+ (D_2^+) and H_3^+ (D_3^+) ions was extracted from a hot filament discharge, accelerated to the desired energy, and momentum analyzed with a 30° bending magnet before entering the experimental chamber. The apparatus within the chamber (Fig. 1) was designed around two rectangular plates, perpendicular to the beam line; an aperture in the first plate (the collector) allowed the beam to pass through to the second plate (the target) from which H^-, H^0, H^+, e^-, as well as sputtered parti-

*Work supported by U. S. Department of Energy, Office of Fusion Energy, under Contract W-7405-ENG-48.

cles were emitted. The collector was used to monitor the negative-ion current, therefore all other charged particles had to be prevented from reaching or leaving it: An electric field between the target and collector plates prevented positive secondary ions from reaching the collector and a transverse magnetic field suppressed secondary electrons. Also, an upbeam collimator shielded the collector from the primary beam. This collimator was the end-plate of a Faraday cup (the collimator-Faraday cup) which was used to determine the total current incident onto the target: The total incident current was determined by the difference in current readings from the collimator-Faraday cup when the beam was deflected into the cup and when it was steered through the cup by a pair of upbeam deflection plates. The H^- (D^-) yields were obtained by taking the ratio of the collector current to the total incident current and dividing by the number of protons (deuterons) per incident molecular ion. A more detailed description of the apparatus is available in the literature.[1]

For H^- yield measurements from thin Li coverage of a W substrate, changes in the surface work function were measured using the retarding potential method.[2,3,4] A W filament could be positioned directly in front of the target, and by measuring the shift in the I-V curves of the diode formed by the filament and the target, the change in the target work function was obtained.

The electric field used to suppress positive ions was produced by applying a negative potential to the target. The magnitude of the applied voltage was determined by the beam species and energy. As an example, a 5.0-keV beam of D_3^+ required a target bias of at least -2.5 kV. The target bias adds to the incident energy giving a total incident energy of 7.5 keV; if we assume that the energy is divided equally between the three deuterons as the incident ion breaks up at the surface, then the maximum energy that a reflected D^+ ion can have is less than 2.5 keV, which is not sufficient for it to reach the collector plate. This explains why, in this experiment, only D_2^+ and D_3^+ were used as incident particles. For D^+ the maximum reflected energy is always greater than the retarding voltage, so that the high-energy backscattered D^+ ions cannot be prevented from reaching the collector.

Clean alkali-metal targets were deposited on a substrate in the cryopumped chamber, which was maintained at a pressure less than 10^{-9} Torr during the measurements. An S.A.E.S. alkali-metal dispenser, mounted on a bellows, could be positioned between the target and collector plates to coat the target area. The thickness of the alkali-metal layer was determined by the current through the dispenser (6 to 8A) and the evaporation time. As an example, passing 7.5A through a Na dispenser for three minutes resulted in the emission of enough Na to form a layer about 15 μm thick (assuming a Na sticking coefficient of unity), which is the same order of magnitude as the average penetration depth of a 1-keV deuteron.[5]

Surface purity was monitored by mass analysis of positive and negative ions sputtered from the surface by the beam. An electrostatic-quadrupole mass analyzer, modified for either positive or negative ions, was placed in the chamber so that it sampled ions leaving the surface at an angle of 50° to the surface normal. Prior to evaporation, many different mass peaks were observed, indicating extensive surface contamination; after a thick alkali-metal target was deposited, the positive-ion spectrum showed only peaks corresponding to sputtered alkali-metal target ions and backscattered incident ions, while the negative ion mass spectrum showed an enhanced $H^-(D^-)$ peak and greatly reduced impurity ion peaks. To determine if the sputtered impurity ions contributed significantly to the total negative ion signal, incident beams of Ar^+ at 4 keV were used. The results showed that the sputtered negative ions contributed less than 5% of the total negative signal on the collector (5% is the limit of measurement).

Results and Discussion

Figure 2 shows the measured H^- yields for Cs, Rb, K, Na and Li targets and Figure 3 shows the measured D^- yields for the same targets as a function of the energy of the incident ions. The estimated standard uncertainties (±10%) incidated in the figures are the result of considering the effects of losses through the collector aperture, D^+ ions leaving the collector, calibration of the electrometers and reproducibility of the measurements.

There are several features worth noting in Figs. 2 and 3:

(1) All the targets show a maximum in the H^- and D^- yields.

(2) The maximum value of the $H^-(D^-)$ yield decreases in the order Cs, Rb, K, Na and Li at any incident energy.

(3) The higher the maximum value of the $H^-(D^-)$ yield, the lower the incident energy at which it occurs.

(4) For any given target the maximum in the D^- yield is less than or equal to the maximum in the H^- yield and occurs at a higher incident energy than the H^- maximum.

(5) The H^- yield per incident proton is the same for H_2^+ and H_3^+ ions incident, and the D^- yield per incident deuteron is the same for D_2^+ and D_3^+ incident, but, at a given incident energy, the D^- and H^- yields are not equal.

Figure 4 shows the H^- yield and the target work function as a function of Li coverage on a W substrate, for 550 eV/p H_3^+ incident. As can be seen from the figure, the H^- yield shows a maximum value of 0.08 per incident proton, corresponding to the minimum value of the work function, 2.1 eV (based upon assigning a work function of 2.5 eV to thick Li). Beyond Li coverage corresponding to the minimum work function, the surface work function rises slowly with increased Li thickness, but the H^- yield decreases rapidly.

The results of these measurements can be interpreted by considering the H^- yield as a function of the probability of reflection of the incident particles, $n(\vec{v})/N_i$, the probability of formation of the H^- ions at the target $P_-(\vec{v})$ and the probability of the survival of the H^- ion as it leaves the target $f(\vec{v})$. The H^- yield is then given by

$$H^- \text{yield} = \frac{1}{N_i} \int_V n(\vec{v}) P_-(\vec{v}) f(\vec{v}) d\vec{v}. \tag{1}$$

If, for the sake of discussion, we assume that the terms are separable,

$$H^- \text{yield} = R_N f P_- \tag{2}$$

where,

R_N is the total particle reflection coefficient

f is the (averaged) probability of H^- survival

P_- is the (averaged) probability of H^- formation.

To discuss the H^- yield measurements in terms of equation (2), we need to know the dependence of R_N, f, P_- on the incident energy. Oen and Robinson[6] have shown that their calculated values of R_N result in a fairly universal curve, independent of projectile and target species, when plotted as a function of reduced energy,* ε. Since ε is proportional to the incident energy, and since R_N is a monotonically decreasing function of ε, R_N is also a monotonically decreasing function of the incident energy.

In the accompanying paper,[7] Hiskes and Schneider shows that P_- is a monotonically decreasing function of the average perpendicular exit velocity, $\langle v_\perp \rangle$, which increases with increasing incident velocity.[6] Similarly, f is a monotonically increasing function of the incident velocity. Therefore, the fact that all the H^- and D^- curves have a maximum at incident energies above about 200 eV indicates that the survival probability is the major factor in determining these yields at incident energies below a few hundred electron volts. Similarly, at high incident energies, the probability of formation and reflection are the factors determining the H^-, D^- yields. Features (2) and (3) above, can be explained by the fact that at the same incident energy the reflection probability decreases in the order given in (3) and that the work function increases in the same order: The lower the work function, the larger the survival probability at lower incident energies, thus shifting the H^-, D^- yield maximum to lower incident energy.

The isotope effect, (4), and (5) arises from the fact that R_N, f, and P_- have different energy dependences. Since ε is almost the same for H and D at the same incident energy, R_N is also the same for both isotopes. However, at the same incident energy, the incident velocity and the aver-

---

*The reduced energy is given by dividing the incident energy by the Lindhard energy, E_L, given by:

$$E_L = \frac{Z_1 Z_2 (M_1 + M_2)(Z_1^{2/3} + Z_2^{2/3})^{1/2}}{a_0 (0.8853) M_2}$$

where subscript 1 = projectiles; subscript 2 = target particles; and a_0 = Bohr radius, [J. Lindhard, M. Scharf and H. E. Schiott, Mat. Fys. Medd. Dan. Vied. Selsk., 33, No. 14 (1963)].

age reflected velocity are higher for H than for D.[6] Thus, at low incident energies, where survival probability dominates, H^- has a higher survival probability and hence a higher yield than D^-. On the other hand, at high incident energies, where formation probability dominates, D^- has a higher formation probability, and thus a higher yield than H^-. This argument also explains the crossing over of the H^- and D^- yield curves. The fact that the isotope effect becomes more pronounced as the target mass and atomic number become smaller is probably due to the mass difference between H and D (1 a.m.u.) becoming more significant compared to the target mass (133 a.m.u. for Cs to 7 a.m.u. for Li), and thus giving rise to different velocity distributions of H^- and D^- leaving the target.

A quantitative discussion of the interpretation of the results is presented by Hiskes and Schneider in the accompanying paper.[7]

References

1. P. J. Schneider, K. H. Berkner, and W. G. Graham, R. V. Pyle, and J. W. Stearns, Proc. of the Symposium on Production and Neutralization of Negative Hydrogen Ions and Beams, Brookhaven 1977, p. 63-69, (LBL report 6839).
2. P. A. Anderson, Phys. Rev., 47, 958 (1935).
3. C. Herring and M. H. Nichols, Rev. Mod. Phys., 21, 185 (1949).
4. J. Millman and S. Seeley, Electronics (McGraw-Hill, New York, 1955), p. 107.
5. J. R. Hiskes, private communication.
6. O. S. Oen and M. T. Robinson, Proc. Sec. Conf. on Surface Effects in Controlled Fusion Devices, San Francisco, CA., 1976 (North Holland Publishing Company, Amsterdam, 1976), p. 210.
7. J. R. Hiskes and P. J. Schneider, this conference.

Figure Captions

Fig. 1. Line drawing of the experimental apparatus.

Fig. 2. H^- yield per incident proton vs. incident energy per proton for H_2^+ and H_3^+ incident on thick alkali-metal targets.

Fig. 3. D^- yield per incident deuteron vs. incident energy per deuteron for D_2^+ and D_3^+ incident on thick alkali-metal targets.

Fig. 4. H^- yield/proton and surface work function vs. Li thickness (arbitrary units) on a W substrate for 550 eV/p H_3^+ incident.

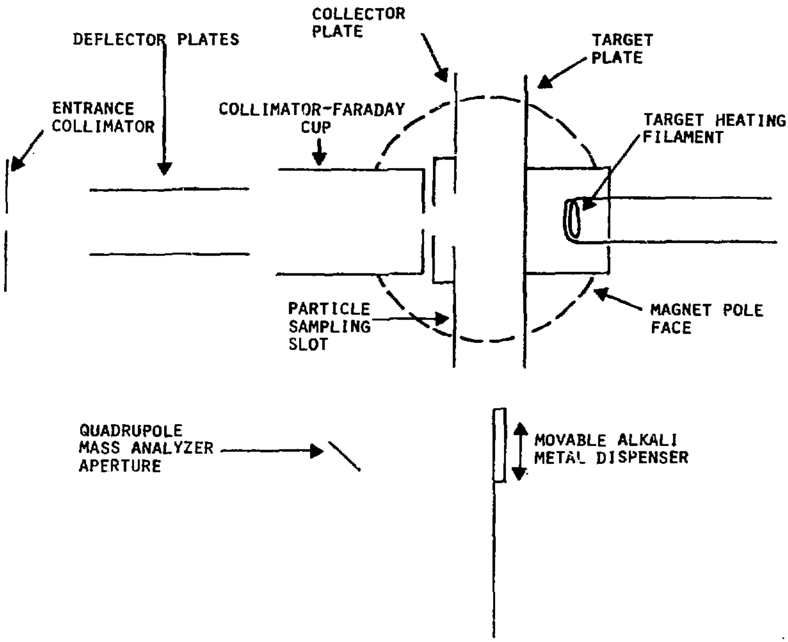

XBL 779-2487

Figure 1

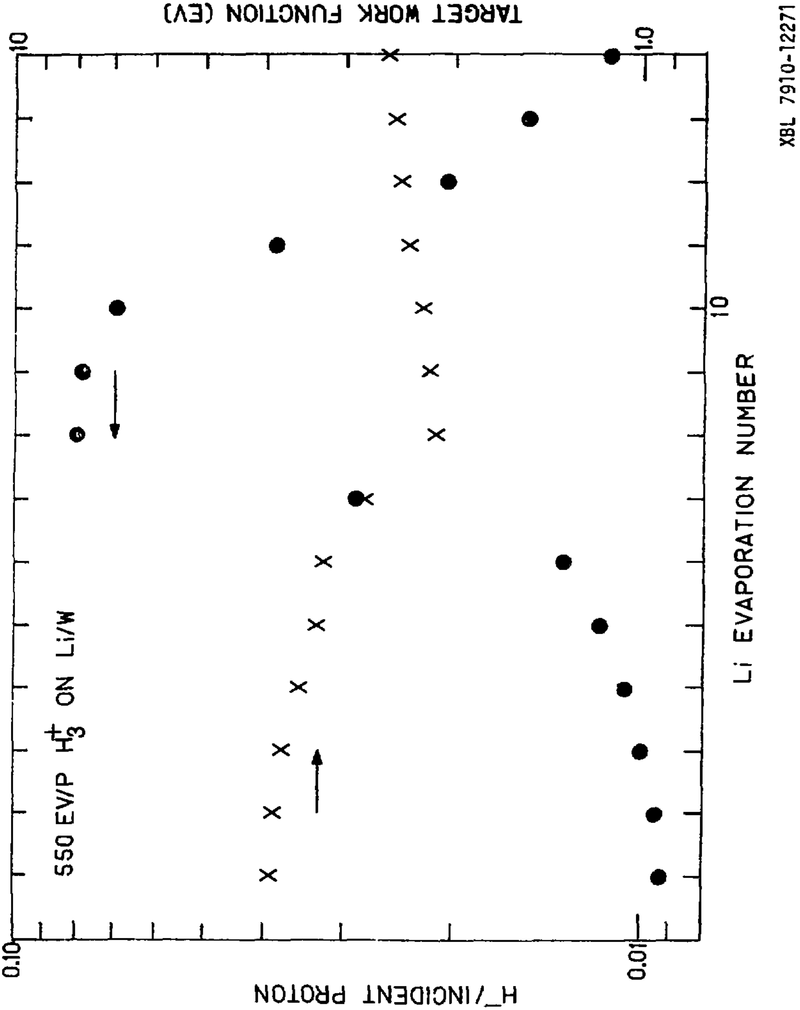
TARGET WORK FUNCTION (EV)
10
1.0
550 EV/P H_3^+ ON Li/W
Li EVAPORATION NUMBER
10
H⁻/INCIDENT PROTON
0.10
0.01
XBL 7910-12271

Figure 4